Brief Communication | Neuroimaging and Head & Neck

https://doi.org/10.3348/kjr.2018.19.1.93
pISSN 1229-6929 · eISSN 2005-8330
Korean J Radiol 2018;19(1):93-100

Korean Journal of Radiology
KJR

In Vivo Assessment of Neurodegeneration in Type C Niemann-Pick Disease by IDEAL-IQ

Ruo-Mi Guo, MD[1, 2*], Qing-Ling Li, MM[3*], Zhong-Xing Luo, MM[1], Wen Tang, MM[1], Ju Jiao, MD[2], Jin Wang, MD[1], Zhuang Kang, MM[1], Shao-Qiong Chen, MD[1], Yong Zhang, MD[1, 2]

Departments of [1]Radiology, [2]Nuclear Medicine, and [3]VIP Medical Center, the Third Affiliated Hospital, Sun Yat-Sen University, Guangzhou 510630, China

Objective: To noninvasively assess the neurodegenerative changes in the brain of patients with Niemann-Pick type C (NPC) disease by measuring the lesion tissue with the iterative decomposition of water and fat with echo asymmetry and least square estimation-iron quantification (IDEAL-IQ).

Materials and Methods: Routine brain MRI, IDEAL-IQ and ^{1}H-proton magnetic resonance spectroscopy (^{1}H-MRS, served as control) were performed on 12 patients with type C Niemann-Pick disease (4 males and 8 females; age range, 15–61 years; mean age, 36 years) and 20 healthy subjects (10 males and 10 females; age range, 20–65 years; mean age, 38 years). The regions with lesion and the normal appearing regions (NARs) of patients were measured and analyzed based on the fat/water signal intensity on IDEAL-IQ and the lipid peak on ^{1}H-MRS.

Results: Niemann-Pick type C patients showed a higher fat/water signal intensity ratio with IDEAL-IQ on T2 hyperintensity lesions and NARs (3.7–4.9%, $p < 0.05$ and 1.8–3.0%, $p < 0.05$, respectively), as compared to healthy controls (HCs) (1.2–2.3%). After treatment, the fat/water signal intensity ratio decreased (2.2–3.4%), but remained higher than in the HCs ($p < 0.05$). The results of the ^{1}H-MRS measurements showed increased lipid peaks in the same lesion regions, and the micro-lipid storage disorder of NARs in NPC patients was detectable by IDEAL-IQ instead of ^{1}H-MRS.

Conclusion: The findings of this study suggested that IDEAL-IQ may be useful as a noninvasive and objective method in the evaluation of patients with NPC; additionally, IDEAL-IQ can be used to quantitatively measure the brain parenchymal adipose content and monitor patient follow-up after treatment of NPC.

Keywords: *Neurodegeneration; Magnetic resonance imaging; Magnetic resonance spectroscopy; Niemann-Pick type C disease*

INTRODUCTION

Niemann-Pick type C (NPC) disease is a hereditary autosomal recessive sphingomyelin lipidosis. An accumulation of lipid-laden macrophages is demonstrable in various tissues such as the central nervous system and/or reticuloendothelial system. In most NPC cases, the neurological defects begin to appear in patients between 4 and 10 years-old (1). The clinical manifestations are usually different and atypical during disease occurrence and development (2-4); hence, NPC diagnosis is often inaccurate and delayed, and death is usually caused by aspiration

Received November 15, 2016; accepted after revision January 1, 2017.
This study was supported by Medical Science Foundation of Guangdong Provence (Grant number: B2014147).
*These authors contributed equally to this work.
Corresponding author: Yong Zhang, MD, Department of Nuclear Medicine, the Third Affiliated Hospital, Sun Yat-Sen University, 600 Tianhe Road, Guangzhou 510630, China.
• Tel: (8620) 85252309 • Fax: (8620) 85253258 • E-mail: zhangyongzssy@126.com
This is an Open Access article distributed under the terms of the Creative Commons Attribution Non-Commercial License (http://creativecommons.org/licenses/by-nc/4.0) which permits unrestricted non-commercial use, distribution, and reproduction in any medium, provided the original work is properly cited.

Copyright © 2018 The Korean Society of Radiology

pneumonia (5, 6).

More recently, the early administration of the neurosteroid, allopregnanolone, showed a significant increase in the life span and a delay in the onset of neurologic deficits in NPC1-/-mice (7). With advances in successful therapies based on animal models, clinical trials with safe, early, reliable, and longitudinal diagnosis in human NPC patients are needed. Magnetic resonance (MR) imaging is a desirable imaging tool for human disease because it is noninvasive and can be performed repeatedly without harmful effects; however, some metabolic and biochemical changes cannot be detected by conventional MR techniques (8). Therefore, new imaging techniques that facilitate sophisticated assessment of cellular metabolism are necessary for further investigation.

Currently, a newly emerging MR technique, iterative decomposition of water and fat with echo asymmetry and least square estimation-iron quantification (IDEAL-IQ), is increasingly used in the research field of lipid metabolism (9, 10); it is a robust method for the quantitative evaluation of tissue fat and provides information on the fat spatial distribution (10, 11). IDEAL-IQ can produce high-resolution, contiguous reconstructed images of fat and water. Fat/water signal ratio images of the entire abdomen have been achieved in the previous studies (9, 10). Because fat metabolism disorder of the brain parenchyma is rare, IDEAL-IQ findings of the brain have rarely been reported. Thus, we used IDEAL-IQ to confirm the diagnosis of NPC, assess the content of lipid storage in the brain parenchymal lesions, and determine its suitability for accurate and non-invasive study of the therapeutic effect and prognosis of lipid storage disorder diseases including NPC. ^{1}H-proton magnetic resonance spectroscopy (^{1}H-MRS), a classic technology in the diagnosis of NPC, was used in conjunction to confirm the reliability of IDEAL-IQ and served as a control (12-14). The purpose of our study was to noninvasively assess the neurodegenerative changes in the brain of patients with NPC disease by IDEAL-IQ.

MATERIALS AND METHODS

Subjects

This was a retrospective study of all MRI brain studies performed in the radiology department from a single institution over a 5 year period between December 2010 and June 2016. Institutional Review Board waiver was obtained prior to the study.

The study was approved by the local research and ethics committee, and the patients gave their informed consent prior to their inclusion in this study. Data were acquired from 12 patients with type C Niemann-Pick disease (4 males and 8 females; age range, 15–61 years; mean age, 36 years) and from 20 healthy subjects (10 males and 10 females; age range, 20–65 years; mean age, 38 years). The control group included healthy subjects with no neurological symptoms. The 12 patients with type C Niemann-Pick disease were referred to our hospital because of clumsiness, ataxia, or mental disturbance without speech, as well as swallowing difficulty that had been progressing rapidly for the past 6 months. Diagnosis was confirmed using the biochemical analysis of cultured fibroblasts (15) and the pathological diagnosis based on a liver biopsy. All study subjects underwent brain MR examination with the IDEAL-IQ and ^{1}H-MRS technologies, on admission and after two months of active treatment. Mini-mental state examinations (MMSE) were used to assess cognitive function for the six patients.

After the 12 patients were admitted to the hospital, their neurological examination revealed apathy, facial grimace, dystonia, clumsiness, mild rigidity in limbs, hyperactive deep tendon reflexes, and limb dysmetria. No retinal pigmentation abnormality was noted by the consulting ophthalmologist. All other physical examination results were normal.

MRI Exploration

All images were produced from a 3T MRI scanner (Discovery 750, GE Healthcare, Milwaukee, WI, USA). Prior to IDEAL-IQ and ^{1}H-MRS, transverse fast spin-echo T_1-weighted sequence (repetition time [TR]/echo time [TE] = 450 ms/12 ms), transverse fast spin-echo T2-weighted sequence (TR/TE = 3800 ms/100 ms), and T2-fluid attenuated inversion recovery (T2-FLAIR) sequence (TR/TE = 9000 ms/140 ms) were recorded (matrix = 256 x 256, field of view [FOV] = 26 x 26 cm, and slice thickness/gap = 5.0 mm/1.0 mm; 24 slices covering the whole brain).

The IDEAL-IQ technique was used on the entire brain in the axial plane, with the following scan parameters: TR = 4 ms, TE = 11.8 ms; bandwidth 125 kHz; echo train length 6; flip angle 5°; number of excitations (NEX) = 1; matrix 256 x 160; and 20 slices at a thickness of 5 mm. Six group images were obtained once the IDEAL-IQ sequence was scanned: in phase image, out of phase image, pure water image, pure fat image, fat/water signal ratio image, and R2* relaxation rate image. The adipose content of the lesion area was directly measured using the fat/water signal ratio image.

Korean Journal of Radiology
KJR

Chemical shift imaging (CSI) was applied in ^{1}H-MRS, and chemical shift selective (CHESS) was used for water suppression. ^{1}H-MRS voxels of interest measuring 20 x 20 x 20 mm^3 were defined in standard locations in the lesions using previously published methods (16). Scanning parameters were: TR/TE = 1000 ms/144 ms, FOV = 24 x 24 cm, phase matrix 18 x 18, slice thickness 5 mm, and NEX = 1. The local magnetic field homogeneity was optimized with the three-plane auto-shim procedure, and the flip angle of the third water suppression pulse was adjusted for CHESS prior to CSI acquisition.

Image Processing

The brain MR images were analyzed by 3 radiologists independently. When the results differed, consensus was reached by discussion. Data of the multi-voxel spectroscopy were transferred to the GE AW4.1 workstation (Sun Microsystems, Santa Clara, CA, USA) for post-processing with research software (FuncTool 6.3.1 software, GE Healthcare). N-acetyl-aspartate (NAA), choline (Cho), creatinine (Cr), lipid (Lip) and lactate (Lac) concentrations, as well as the NAA/Cr ratio and the Cho/Cr ratio, were measured. The Lip signal was a single peak (0.9 ppm), and inverted double peak of Lac signal was seen at 1.33 ppm. The IDEAL-IQ datasets were transferred to the workstation and processed using Functool 6.3.1 software. The box-shaped regions of interest (ROIs) were defined as the average of three replicates each in the area of signal intensity change on T2-FLAIR imaging sequences corresponding to a voxel of interest in the CSI data by each observer in succession. The same range of the surrounding or contralateral normal appearing regions (NARs) were selected as the controls at the same level image of the lesion. The average size of the ROIs was 1 cm^2, with variation based on the lesion range. The same location-matched fat/water signal ratios were quantitatively measured in lesion regions, NARs in NPC patients, and the healthy controls (HCs).

Statistical Analysis

All data were expressed as the means ± standard deviation, unless stated otherwise, and the number of measurements was 28 for each patient. The fat/water signal ratio was compared between HCs and lesion tissues in the patient groups by using a repeated-measures one-way analysis of variance test, followed by Kruskall-Wallis test for multiple pairwise comparisons among different times. Statistical calculations were performed with SPSS 12.0 software for Windows (SPSS Inc., Chicago, IL, USA). All p values of < 0.05 were considered as statistically significant difference.

RESULTS

The main symptom of the 12 NPC patients at admission was clumsiness (12 cases, 100%), and the most common signs during hospitalization were apathy (9 patients, 75.0%) and facial grimace (7 patients, 58.3%). In addition, the MMSE scores were abnormal in all patients (Table 1). One patient with the lowest MMSE score deteriorated further despite active treatment, and soon died; the other 11 patients gradually recovered after 2 months without significant intellectual or neurologic deficits. The neurological examinations and MMSE scores were all normal in the HCs.

Table 1. Clinical Data and MMSE Scores of Niemann-Pick Type C Patients

Age (y)/Sex	Symptoms on Admission	Signs During Hospitalization	MMSE Scores
26/Female	Clumsiness, ataxia	Apathy, dystonia, and clumsiness	25
35/Male	Clumsiness, ataxia	Apathy, facial grimace, and limb dysmetria	16
15/Female	Clumsiness	Facial grimace, and clumsiness	22
42/Male	Clumsiness, mental disturbance	Apathy, dystonia, and hyperactive deep tendon reflexes	13
37/Female	Clumsiness, ataxia	Apathy, facial grimace, and limb dysmetria	18
61/Female	Clumsiness, mental disturbance	Apathy, facial grimace, and mild rigidity in limbs	8*
39/Male	Clumsiness, ataxia	Apathy, facial grimace	17
36/Female	Clumsiness	Apathy, limb dysmetria	18
32/Male	Clumsiness, ataxia	Hyperactive deep tendon reflexes	22
55/Female	Clumsiness, ataxia	Apathy, limb dysmetria	25
38/Female	Clumsiness, mental disturbance	Apathy, facial grimace	13
41/Female	Clumsiness	Facial grimace, and clumsiness	22

*Patient deteriorated further despite active treatment, and soon died. MMSE = mini-mental state examinations

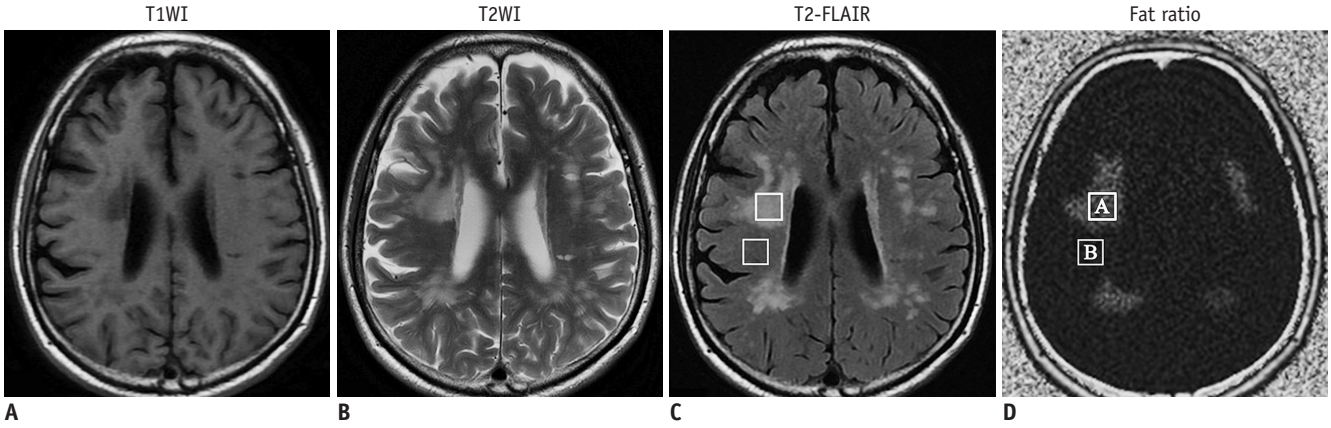

Fig. 1. 35-year-old man with apathy, facial grimace, and limb dysmetria.
Axial T1WI show hypo-intense signal **(A)**, and axial T2WI **(B)** and T2-FLAIR image **(C)** show bilateral hyper-intensities in frontal-parietal periventricular white matters and corona radiata. Fat/water signal ratios of lesion (value A is 4.6) and surrounding normal appearing regions (value B is 2.9) in right corona radiata are measured from fat/water signal ratio image **(D)**. T1WI = T1-weighted image, T2-FLAIR = T2-fluid attenuated inversion recovery, T2WI = T2-weighted image

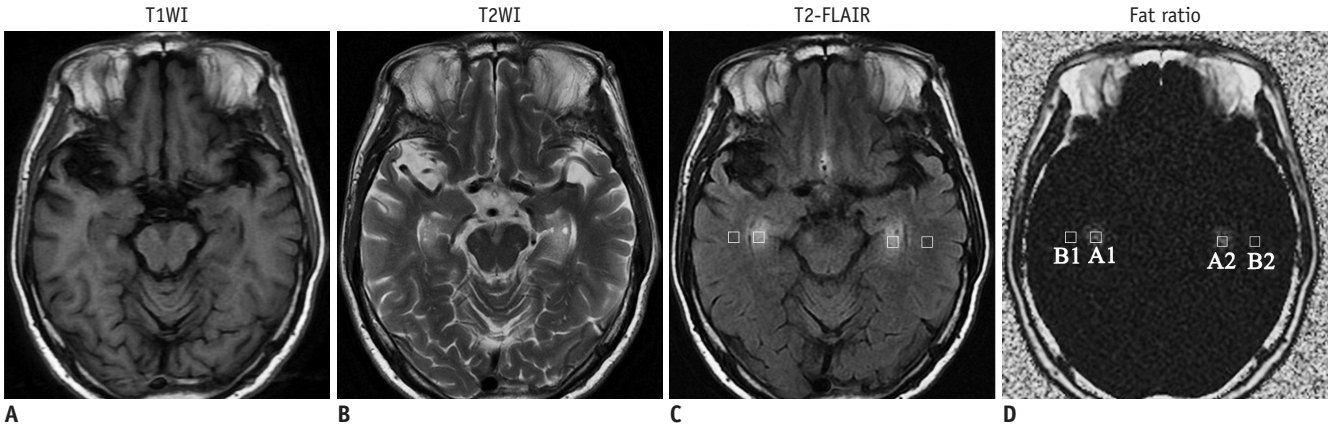

Fig. 2. 42-year-old man with apathy, dystonia, and hyperactive deep tendon reflexes.
Axial T1WI show hypo-intense signal **(A)**, and axial T2WI **(B)** and T2-FLAIR image **(C)** show unilateral hyper-intensities in left frontal periventricular white matters. The fat/water signal ratios of lesion (value A is 4.5) and contralateral normal appearing regions (value B is 1.7) are measured from fat/water signal ratio image. A1, A2, B1, and B2 is regions of interest for measuring lipid content in hyperintensities areas **(D)**.

Detailed MRI data were available for all subjects. No lesions were found in the white matter or the other parts of the brain in the HCs. Bilateral involvement of the frontal-parietal periventricular white matter was observed as hyper-intensities in 10 patients (83.3%) on T2-weighted and T2-FLAIR imaging sequences (Fig. 1). Additional involvement of the corona radiata, centrum semiovale, frontal, temporal, or occipital cortices was observed in 12 patients, although it was much more variable in extent and location (Figs. 1, 2). Four patients (33.3%) showed bilateral hyper-intensities in the hippocampal region. Twelve patients manifested various degrees of enlargement of the ventricles and various ranges of atrophy of the cerebrum and cerebellum, particularly in the frontal lobes (Figs. 1, 2).

The fat/water signal ratios of lesions were increased in fat/water signal ratio on images from the IDEAL-IQ sequence (Figs. 1, 2) on admission, as compared with the fat/water signal ratios of surrounding or contralateral normal area. In NPC patients, the same location-matched fat/water signal ratios were 1.2–2.3% in the HCs (Fig. 3), and the fat/water signal ratio values were significantly lower than those of lesions (3.7–4.9%, $p < 0.05$), and NARs (1.8–3.0%, $p < 0.05$). The fat/water signal ratios of lesion regions were decreased (2.2–3.4%) with the gradual recovery of NPC patients after 2 months of active treatment (Fig. 4), but remained higher than HCs ($p < 0.05$).

The ^{1}H-MRS of the same location-matched lesion regions showed reduction in NAA/Cr resonance intensity and an increase in the Cho signal, the Lip signal and the Lac signal, and the quantitative data of lipid peak; and IDEAL-

Korean Journal of Radiology
KJR

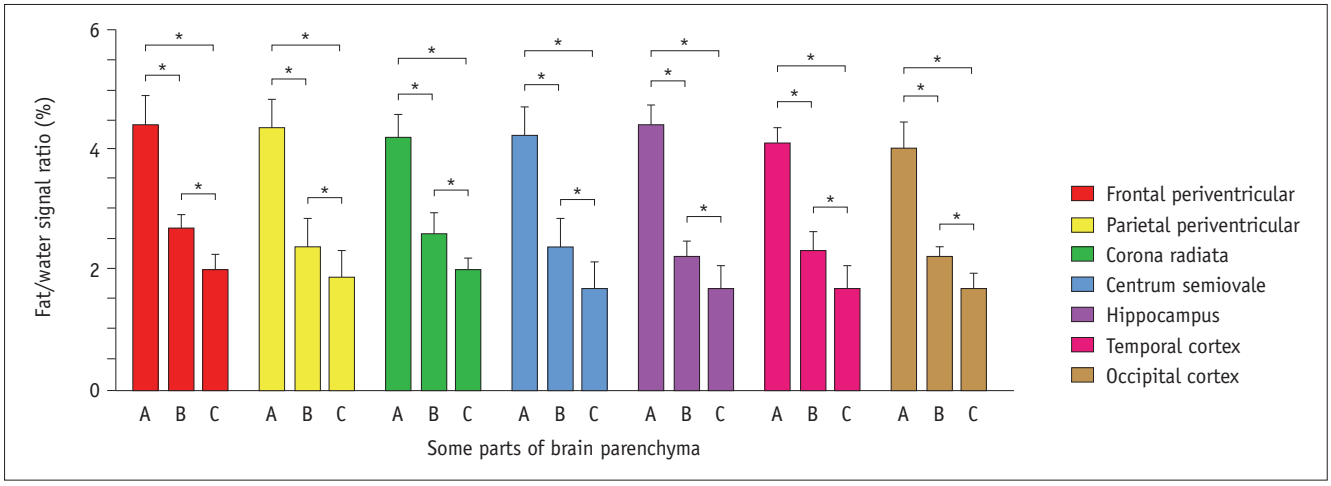

Fig. 3. Fat/water signal ratios of multiple parenchymal parts including frontal periventricular, parietal periventricular, corona radiata, centrum semiovale, hippocampus, temporal and occipital cortex in all subjects were quantitatively measured in fat/water signal ratio image of iterative decomposition of water and fat with echo asymmetry and least square estimation-iron quantification sequence. Fat/water signal ratios of lesion regions (A) are higher than those of NARs in NPC group (B) and control group (C). In addition, fat/water signal ratios were also increased slightly in NARs of NPC group (B) than control group (C). *$p < 0.05$ compared with NARs in NPC group or control group, and compared between NARs in NPC group and control group. A = lesion regions in NPC group, B = normal appearing regions in NPC group, C = normal appearing regions in control group, NARs = normal appearing regions, NPC = Niemann-Pick type C disease

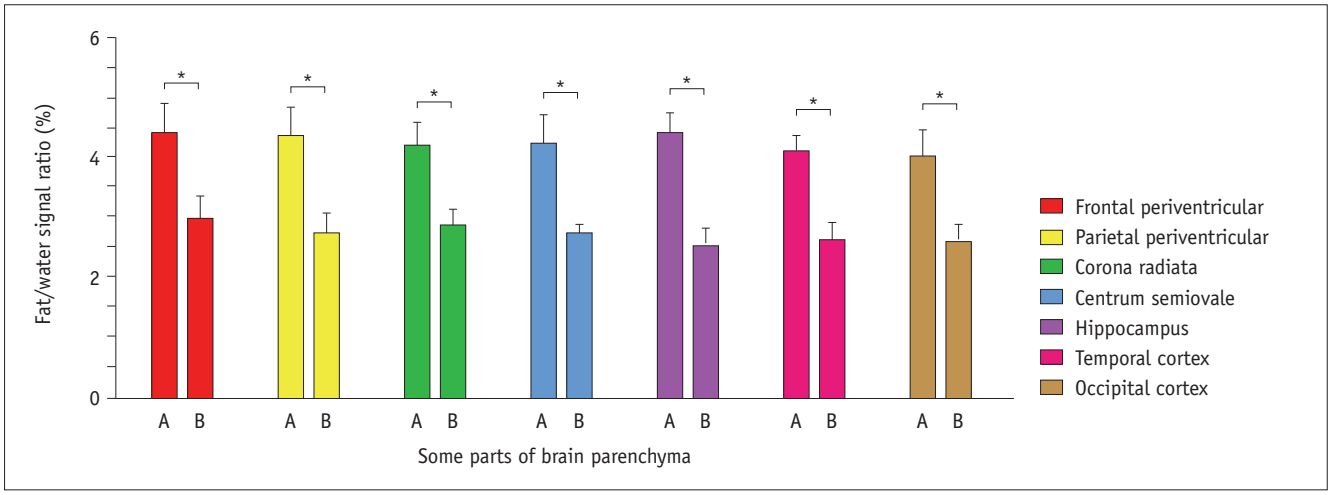

Fig. 4. Fat/water signal ratios of multiple parenchymal parts including frontal periventricular, parietal periventricular, corona radiata, centrum semiovale, hippocampus, temporal and occipital cortex in all subjects were quantitatively measured in fat/water signal ratio image of iterative decomposition of water and fat with echo asymmetry and least square estimation iron quantification sequence on admission and after two months. Fat/water signal ratios of lesion regions on admission (A) are higher than same location-matched fat/water signal ratios after two months (B). *$p < 0.05$ compared with same location-matched fat/water signal ratios after two months. A = lesion regions on admission, B = lesion regions after two months

IQ parameters in the same location-matched lesion regions and NARs showed normal values or were undetectable in the NARs and HCs on admission (Fig. 5), and the micro-lipid storage disorder of NARs in NPC patient was detectable by IDEAL-IQ instead of ^{1}H-MRS (Fig. 6).

DISCUSSION

Niemann-Pick type C disease is a rare autosomal recessive lipid storage disorder caused by impaired cellular functions in processing and transporting low-density lipoprotein-cholesterol. Patients predominantly exhibiting apathy and facial grimace displayed a reduction of brain parenchyma and cortical atrophy predominating in the frontal lobes; these deficits reflect a decrease in the number of neurons. In addition, patients with predominantly gait and movement disorders showed cerebellar atrophy, with relative sparing of the cortical and subcortical areas.

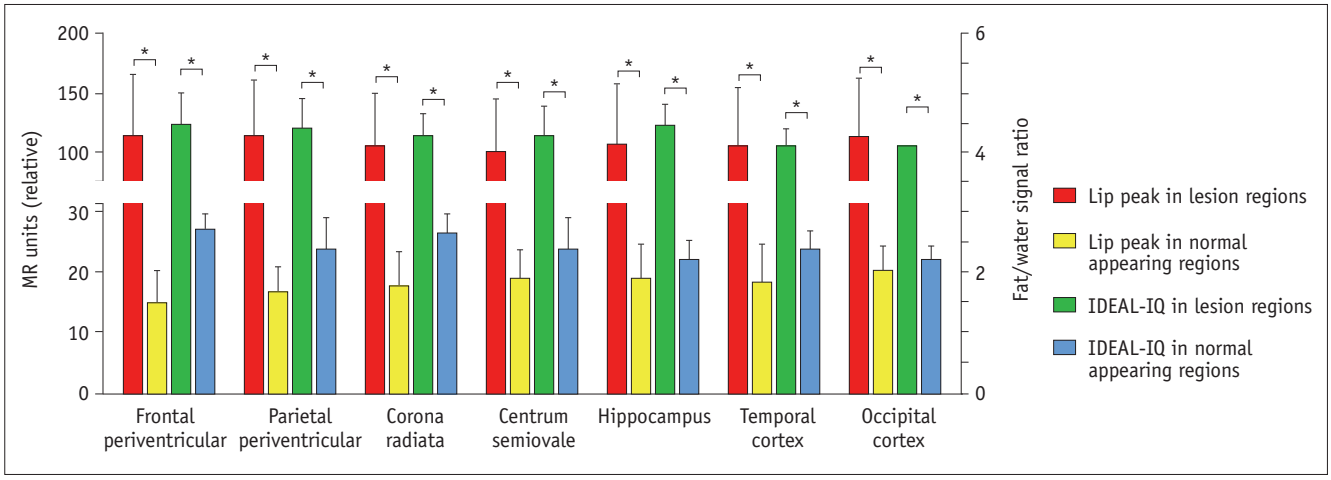

Fig. 5. Lipid peak and fat/water signal ratios of multiple parenchymal parts including frontal periventricular, parietal periventricular, corona radiata, centrum semiovale, hippocampus, temporal and occipital cortex in NPC group were quantitatively measured in ^{1}H-proton magnetic resonance spectroscopy and fat/water signal ratio image of IDEAL-IQ sequence on admission. Quantitative data of lipid peak (left Y axis) in lesion regions are higher than those in NARs, and fat/water signal ratios (right Y axis) of same location-matched lesion regions are higher than those of same location-matched NARs in NPC group. *p < 0.05 compared with NARs in NPC group, normal appearing regions in NPC group. IDEAL-IQ = iterative decomposition of water and fat with echo asymmetry and least square estimation-iron quantification, Lip = lipid

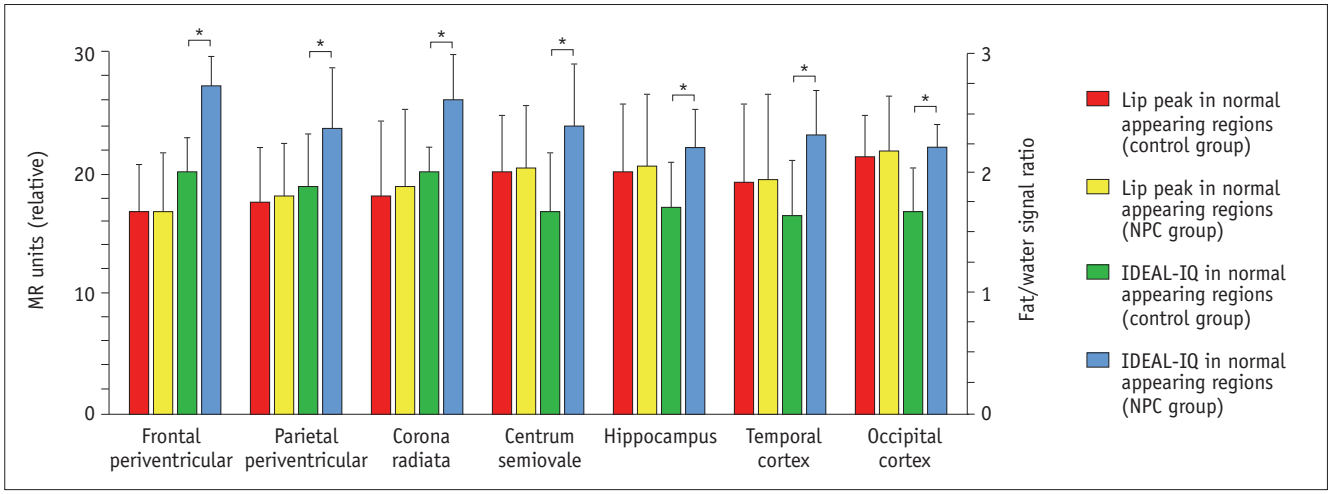

Fig. 6. Lipid peak and fat/water signal ratios of multiple parenchymal parts including frontal periventricular, parietal periventricular, corona radiata, centrum semiovale, hippocampus, temporal and occipital cortex in all subjects were quantitatively measured in ^{1}H-proton magnetic resonance spectroscopy and fat/water signal ratio image of IDEAL-IQ sequence. Fat/water signal ratios (right Y axis) of NARs in NPC group are higher than those of control group. Additionally, quantitative data of lipid peak (left Y axis) showed no significant difference between NARs of NPC and control groups. *p < 0.05 compared between NARs in NPC group and control group.

To the best of our knowledge, the IDEAL-IQ findings in NPC patients have not been reported. Our findings from the IDEAL-IQ sequence analysis demonstrated that NPC patients exhibit markedly higher fat/water signal ratios in lesion regions, as compared with those of the NARs. Thus, changes in the lesions might not be only a metabolic functional change, which speeds up the deposition of sphingomyelin and cholesterol in the brain tissue; they may also cause significant micro-structural damage of neurons and the myelin sheath during the disease course (17-19). In addition, the fat/water signal ratios were also slightly increased in the NARs of NPC group, as compared to those of the control group. Thus, the NARs of NPC patients, without the benefit of routine brain MR imaging, may already have pathological changes at the molecular level.

The decreased fat/water signal ratios in lesion regions after 2 months of active treatment may be due to the recovery of metabolic function from the decomposition

Korean Journal of Radiology
KJR

of sphingomyelin and cholesterol in the brain tissue; in addition, the IDEAL-IQ can be used to quantitatively measure and monitor the brain-parenchymal adipose content at different stages of lipid storage disorder diseases.

The IDEAL-IQ technology has been used in the breast, abdomen, and spine (9, 11, 20), but there is a lack of reports on its use in the brain for rare fat metabolism disorders. In this study, we used the IDEAL-IQ to study the lipid storage disorder of the brain parenchyma and compare the fat/water signal ratios measured in lesions and in NARs in the NPC and control groups. The regions were also evaluated and confirmed by ^{1}H-MRS based on the degree of abnormality of NAA/Cr, Cho/Cr and the presence of an abnormal Lip and Lac peak. Compared with the qualitative and semi-quantitative diagnosis of the ^{1}H-MRS, the IDEAL-IQ not only enables a qualitative diagnosis but also can quantitatively measure the degree of disease and provide guidance for the treatment and prognosis of the NPC. However, the sensitivity of the ^{1}H-MRS is not as good as that of IDEAL-IQ in detecting micro-lipid storage disorder of NARs in NPC patients. Furthermore, IDEAL-IQ might be useful for noninvasively monitoring disease progression and response to therapy in cases with different lesions, processes, and local adipose content.

Our study has a few limitations. First, a small number of subjects were included, and further large sample of study is needed. Second, there was lack of quantitative correlation of IDEAL-IQ parameters with lipid peak on MR spectroscopy (i.e., using LC model). Third, lack of inter- or intra-observer reliability needs to be discussed.

In conclusion, IDEAL-IQ is a novel tool for non-invasive and objective evaluation of the lipid storage disorder of patients with NPC. The sensitivity of IDEAL-IQ is better than that of ^{1}H-MRS in detecting micro-lipid storage disorder of NARs in NPC patients. The brain parenchymal adipose content in NPC can be quantitatively measured using the IDEAL-IQ in real time as well as in post-treatment follow-up. Further studies in more NPC patients and patients with other neurodegenerative are needed to verify our findings.

Acknowledgments

The authors thank the participants of this study, magnetic resonance technicians of my department for their technical assistance.

REFERENCES

1. Yang CC, Su YN, Chiou PC, Fietz MJ, Yu CL, Hwu WL, et al. Six novel NPC1 mutations in Chinese patients with Niemann-Pick disease type C. *J Neurol Neurosurg Psychiatry* 2005;76:592-595
2. Brady RO, Filling-Katz MR, Barton NW, Pentchev PG. Niemann-Pick disease types C and D. *Neurol Clin* 1989;7:75-88
3. Fink JK, Filling-Katz MR, Sokol J, Cogan DG, Pikus A, Sonies B, et al. Clinical spectrum of Niemann-Pick disease type C. *Neurology* 1989;39:1040-1049
4. Vanier MT. Phenotypic and genetic heterogeneity in Niemann-Pick disease type C: current knowledge and practical implications. *Wien Klin Wochenschr* 1997;109:68-73
5. Imrie J, Vijayaraghaven S, Whitehouse C, Harris S, Heptinstall L, Church H, et al. Niemann-Pick disease type C in adults. *J Inherit Metab Dis* 2002;25:491-500
6. Sévin M, Lesca G, Baumann N, Millat G, Lyon-Caen O, Vanier MT, et al. The adult form of Niemann-Pick disease type C. *Brain* 2007;130:120-133
7. Griffin LD, Gong W, Verot L, Mellon SH. Niemann-Pick type C disease involves disrupted neurosteroidogenesis and responds to allopregnanolone. *Nat Med* 2004;10:704-711
8. Park M, Moon WJ. Structural MR imaging in the diagnosis of Alzheimer's disease and other neurodegenerative dementia: current imaging approach and future perspectives. *Korean J Radiol* 2016;17:827-845
9. Ma J, Song Z, Yan F. Detection of hepatic and pancreatic fat infiltration in type II diabetes mellitus patients with IDEAL-Quant using 3.0T MR: comparison with single-voxel proton spectroscopy. *Chin Med J (Engl)* 2014;127:3548-3552
10. Kim H, Taksali SE, Dufour S, Befroy D, Goodman TR, Petersen KF, et al. Comparative MR study of hepatic fat quantification using single-voxel proton spectroscopy, two-point dixon and three-point IDEAL. *Magn Reson Med* 2008;59:521-527
11. Hofstetter LW, Yeo DT, Dixon WT, Kempf JG, Davis CE, Foo TK. Fat-referenced MR thermometry in the breast and prostate using IDEAL. *J Magn Reson Imaging* 2012;36:722-732
12. Tedeschi G, Bonavita S, Barton NW, Betolino A, Frank JA, Patronas NJ, et al. Proton magnetic resonance spectroscopic imaging in the clinical evaluation of patients with Niemann-Pick type C disease. *J Neurol Neurosurg Psychiatry* 1998;65:72-79
13. Galanaud D, Tourbah A, Lehéricy S, Leveque N, Heron B, Billette de Villemeur T, et al. 24 month-treatment with miglustat of three patients with Niemann-Pick disease type C: follow up using brain spectroscopy. *Mol Genet Metab* 2009;96:55-58
14. Sylvain M, Arnold DL, Scriver CR, Schreiber R, Shevell MI. Magnetic resonance spectroscopy in Niemann-Pick disease type C: correlation with diagnosis and clinical response to cholestyramine and lovastatin. *Pediatr Neurol* 1994;10:228-232
15. Zaaraoui W, Crespy L, Rico A, Faivre A, Soulier E, Confort-Gouny S, et al. In vivo quantification of brain injury in adult Niemann-Pick disease Type C. *Mol Genet Metab* 2011;103:138-141
16. Robertson DM, van Amelsvoort T, Daly E, Simmons

A, Whitehead M, Morris RG, et al. Effects of estrogen replacement therapy on human brain aging: an in vivo 1H MRS study. *Neurology* 2001;57:2114-2117
17. Harzer K, Schlote W, Peiffer J, Benz HU, Anzil P. Neurovisceral lipidosis compatible with Niemann-Pick disease type C: morphological and biochemical studies of a late infantile case and enzyme and lipid assays in a prenatal case of the same family. *Acta Neuropathol* 1978;43:97-104
18. Ong WY, Kumar U, Switzer RC, Sidhu A, Suresh G, Hu CY, et al. Neurodegeneration in Niemann-Pick type C disease mice. *Exp Brain Res* 2001;141:218-231
19. German DC, Liang CL, Song T, Yazdani U, Xie C, Dietschy JM. Neurodegeneration in the Niemann-Pick C mouse: glial involvement. *Neuroscience* 2002;109:437-450
20. Ren AJ, Guo Y, Tian SP, Shi LJ, Huang MH. MR imaging of the spine at 3.0T with T2-weighted IDEAL fast recovery fast spin-echo technique. *Korean J Radiol* 2012;13:44-52